Energetics of Uracil Cation Radical and Anion Radical Ion−Molecule Reactions in the Gas Phase

František Tureček* and Jill K. Wolken

Department of Chemistry, Bagley Hall, Box 351700, University of Washington, Seattle, Washington 98195-1700

Received: May 4, 2001; In Final Form: July 9, 2001

The uracil cation radical was calculated to exist predominantly as the 1,3-dioxo tautomer $\mathbf{1}^{\bullet+}$, similar to the most stable tautomer of neutral uracil (**1**). The enol forms of $\mathbf{1}^{\bullet+}$ were found to be 10−173 kJ mol^{-1} less stable than $\mathbf{1}^{\bullet+}$ and should not be significantly populated at 298 K thermal equilibrium. Cation radical $\mathbf{1}^{\bullet+}$ is a moderately strong gas-phase acid of topical acidities ΔH_{acid} = 829, 921, 916, and 879 kJ mol^{-1} for the H-1, H-3, H-5, and H-6 protons, respectively. Ion $\mathbf{1}^{\bullet+}$ is capable of exothermic protonation of adenine, guanine, and cytosine, and of the arginine, lysine, histidine, and tryptophan amino acid residues in proteins. The hydrogen atom affinities of $\mathbf{1}^{\bullet+}$ were $-\Delta H_{rxn}$ = 432, 371, and 360 kJ mol^{-1} for H-atom additions to O-4, O-2, and C-5, respectively. $\mathbf{1}^{\bullet+}$ was calculated to exothermically abstract the thiol hydrogen atom from CH_3SH, the hydroxyl hydrogen from phenol, and an α-hydrogen atom from glycine *N*-methylamide. Uracil radicals formed by deprotonation of $\mathbf{1}^{\bullet+}$ were calculated to have large hydrogen atom affinities that should allow for exothermic abstraction of H-atoms from thiol groups, phenolic hydroxyls, and amino acid backbone α-methylene and methine groups. Protonation by a uracil cation radical followed by hydrogen atom abstraction can propagate radiation damage from the initial ionization site. In contrast to the highly reactive uracil cation radicals and radicals, the weakly bound uracil anion radical ($\mathbf{1}^{\bullet-}$) was predicted to be much less reactive in the gas phase. Ion−molecule reactions of $\mathbf{1}^{\bullet-}$ by proton and hydrogen atom abstractions from thiols, phenol, and α-positions of amino acids were calculated to be endothermic and thus very slow in the gas phase. $\mathbf{1}^{\bullet-}$ can selectively deprotonate carboxylic groups as calculated for the reaction with glycine.

Introduction

Radiation damage in DNA and RNA occurs by direct or indirect action of high-energy photons or electrons on the nucleobase and, to a lesser extent, carbohydrate residues.[1] In the direct mechanism, the nucleobase is ionized by the radiation to form a cation radical.[1,2] The latter is a highly reactive species in the condensed phase that undergoes a variety of reactions that can chemically modify the nucleobase itself and the surrounding chemical moieties. In the indirect mechanism, the nucleobase captures a thermal electron produced by primary ionization to form an anion radical.[3] Further reactions of the anion radical then can result in chemical modifications of the nucleobase or other chemical moieties in the vicinity of the anion radical. Although redox and addition reactions of nucleobase radicals and ions have been studied extensively in aqueous solution as reviewed,[2] there are no reliable data on the reaction energetics. The gas phase represents a suitable reference medium in which the reaction energetics can be established in the absence of solvent effects and other interferences. There have been recent reports on ion−molecule reactions of gas-phase nucleobase cation radicals with several neutral counterparts[4a] and neutral nucleobases with gas-phase radical cations that showed electron and proton transfer as well as radical addition reactions.[4b] However, thermochemical data are currently unavailable for most ion−molecule reactions of interest to gas-phase ion chemistry and radiation damage. In this paper we examine by high-level ab initio calculations the energetics of gas-phase reactions of the cation radical and anion radical of the RNA nucleobase uracil. The reactions studied here comprise proton, hydrogen atom, hydride, and methanethiyl radical transfers. These reactions model interactions of nucleobase ion radicals with neutral nucleobases and also with the peptide backbone and amino acid side chains in proteins containing cysteine, cystine, and tyrosine residues that are considered the prime targets for radical-induced DNA− or RNA−protein reactions.[1]

Calculations

Standard ab initio and density functional theory calculations were performed using the Gaussian 98 suite of programs.[5] Geometries were optimized using Becke's hybrid functional (B3LYP)[6] and the 6-31+G(d,p) basis set. Spin-unrestricted calculations (UB3LYP) were used for open-shell systems. Spin contamination in the UB3LYP calculations was small as judged from the $\langle S^2 \rangle$ operator expectation values that were 0.75−0.77. The optimized structures were characterized by harmonic frequency analysis as local minima (all frequencies real) or first-order saddle points (one imaginary frequency). Complete optimized structures in the Cartesian coordinate format and total energies are available from the corresponding author (F. T.) upon request. The B3LYP/6-31+G(d,p) frequencies were scaled by 0.963 (ref 7; for other scaling factors see ref 8) and used to calculate zero-point vibrational energies (ZPVE) and enthalpy corrections. The rigid-rotor harmonic oscillator approximation was used in all thermochemical calculations. Single-point energies were calculated at several levels of theory. In two sets

* Corresponding author. Telephone: (206) 685-2041. Fax: (206) 685-3478. E-mail: turecek@chem.washington.edu.

10.1021/jp0116860 CCC: $20.00
Published on Web 09/01/2001

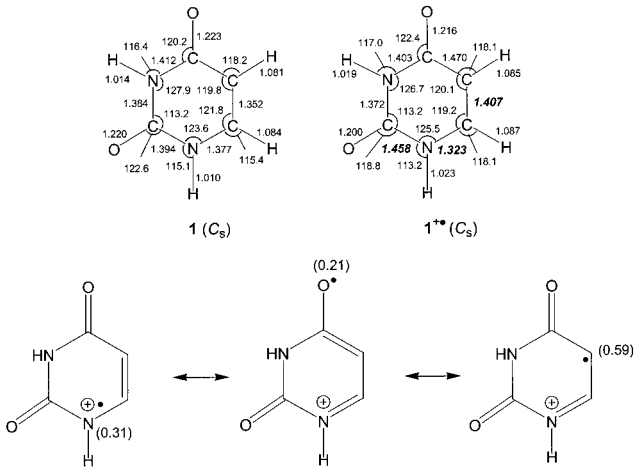

Figure 1. B3LYP/6-31+G(d,p) optimized geometries of **1** and $\mathbf{1}^{\bullet+}$. Bond lengths in angstroms, bond and dihedral angles in degrees. The bold italic numerals highlight the bond lengths that change most upon ionization. Atomic spin densities from B3LYP/6-311+G(2d,p) calculations are shown in parentheses in the canonic structures.

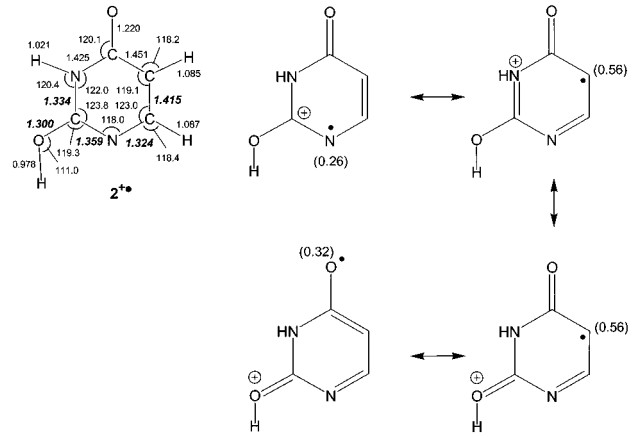

Figure 2. B3LYP/6-31+G(d,p) optimized geometry of $\mathbf{2}^{\bullet+}$. Bond lengths in angstroms, bond and dihedral angles in degrees. The bold italic numerals highlight the bond lengths that change most upon ionization. Atomic spin densities from B3LYP/6-311+G(2d,p) calculations are shown in parentheses in the canonic structures.

of calculations, MP2(frozen core)[9] and B3LYP energies were calculated with basis sets of increasing size, e.g., 6-311+G(2d,p) and 6-311+G(3df,2p). Spin contamination in the UMP2 calculations was moderate for uracil radicals and transition states, as evidenced by the spin expectation values $\langle S^2 \rangle$ that ranged between 0.76 and 0.91. Spin annihilation using Schlegel's projection method[10] (PMP2)[5] reduced the $\langle S^2 \rangle$ values to 0.75−0.76. The PMP2 energies were averaged with the B3LYP energies according to the empirical procedure that was introduced previously[11] and tested for several systems since.[12,13] This resulted in error cancellation and provided relative energies denoted as B3-PMP2. Calculations on closed-shell systems are marked by B3-MP2. In addition, a composite procedure was adopted that consisted of a single-point quadratic configuration interaction calculation,[14] QCISD(T)/6-31G(d,p), and basis set expansion up to 6-311+G(3df,2p) through PMP2 or ROMP2 single-point calculations according to eq 1:

$$\text{QCISD(T)/6-311+G(3df,2p)} \approx \text{QCISD(T)/6-31G(d,p)} + \text{MP2/6-311+G(3df,2p)} - \text{MP2/6-31G(d,p)} \quad (1)$$

This level of theory is intermediate between those of the Gaussian 2 (MP2) method[15] which uses the 6-311G(d,p) basis

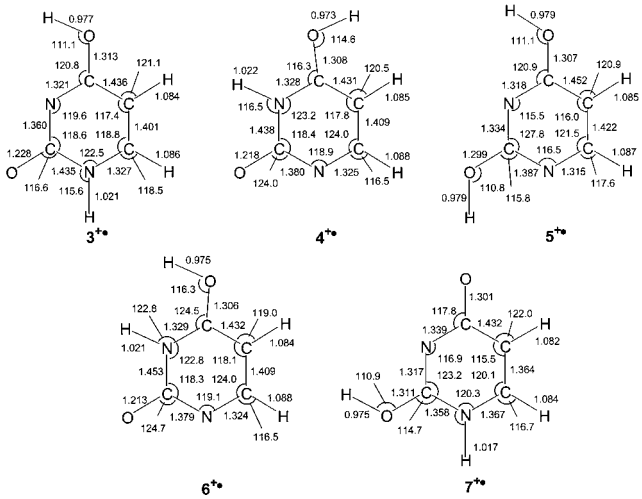

Figure 3. B3LYP/6-31+G(d,p) optimized geometries of $\mathbf{3}^{\bullet+}-\mathbf{7}^{\bullet+}$. Bond lengths in angstroms, bond and dihedral angles in degrees.

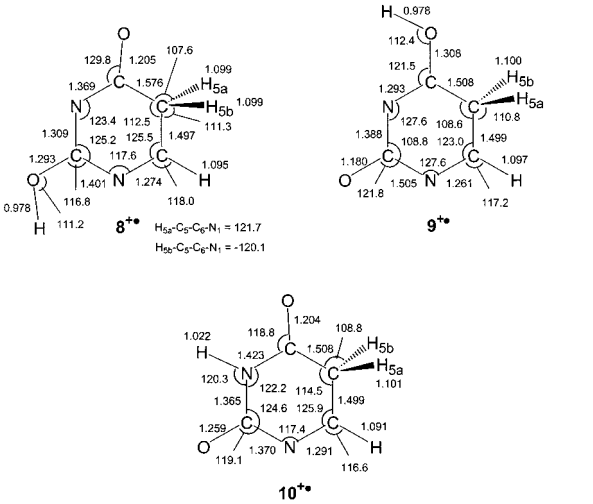

Figure 4. B3LYP/6-31+G(d,p) optimized geometries of $\mathbf{8}^{\bullet+}-\mathbf{10}^{\bullet+}$. Bond lengths in angstroms, bond and dihedral angles in degrees.

set in the large QCISD(T) calculation and the G2(MP2,SVP) method[16] which uses the 6-31G(d) basis set instead. The calculated total energies are available from the corresponding author upon request.

Results and Discussion

Properties of Uracil Cation Radicals. Several tautomeric structures were found for uracil cation radicals ($\mathbf{1}^{\bullet+}-\mathbf{10}^{\bullet+}$) to exist as local energy minima, a situation which is closely similar to that for the tautomers of neutral uracil.[17] It is therefore instructive to discuss the structures and relative energies of cation radical tautomers with reference to the neutral tautomers. The B3LYP/6-31+G(d,p) optimized geometry of the most stable ion tautomer $\mathbf{1}^{\bullet+}$ was generally similar to that of the most stable neutral tautomer **1** (Figure 1). However, there were notable differences in the N-1−C-2 and C-5−C-6 bonds that were longer in $\mathbf{1}^{\bullet+}$ than in **1**, whereas the N-1−C-6 bond was shorter in the ion (Figure 1). The bonds in $\mathbf{1}^{\bullet+}-\mathbf{10}^{\bullet+}$ that differed most from those in the corresponding neutral tautomers are highlighted as bold italics in Figures 1−4. The changes in bond lengths upon ionization, $\mathbf{1} \rightarrow \mathbf{1}^{\bullet+}$, can be attributed to the different bond orders in the ion, as visualized by the canonical structures and documented by the atomic spin densities from B3LYP/6-311+G(2d,p) calculations (values in parentheses,

TABLE 1: Relative Energies of Uracil Cation Radical Tautomers

	relative energy[a]								
ion	B3LYP/ 6-31+ G(d,p)	B3LYP/ 6-311+ G(2d,p)	B3-PMP2[b]/ 6-311+ G(2d,p)	PMP2/ 6-311+ G(2d,p)	QCISD(T)/ 6-311+ G(2d,p)	B3LYP/ 6-311+ G(3df,2p)	B3-PMP2/ 6-311+ G(3df,2p)[b]	PMP2/ 6-311+ G(3df,2p)	QCISD(T)/ 6-311+ G(3df,2p)[c]
1$^{\bullet+}$	0	0	0	0	0	0	0	0	0
2$^{\bullet+}$	6	7	10	13	8	7	10	13	8 (7.7)[d]
3$^{\bullet+}$	24	23	26	29	29	24	27	29	30 (29.3)[d]
4$^{\bullet+}$	42	41	44	47					
5$^{\bullet+}$	42	40	46	52					
6$^{\bullet+}$	49	47	51	54					
7$^{\bullet+}$	48	48	55	62					
8$^{\bullet+}$	151	147	148	150					
9$^{\bullet+}$	144	142	159	175					
10$^{\bullet+}$	156	155	173	191					

[a] In units of kJ mol^{-1} at 0 K. [b] From averaged B3LYP and PMP2 energies. [c] Effective energies from eq 1. [d] 298 K relative enthalpies.

TABLE 2: Energetics of Uracil Cation and Radical Reactions

	relative energy[a]								
reaction	B3LYP/ 6-31+ G(d,p)	B3LYP/ 6-311+ G(2d,p)	B3-PMP2/ 6-311+ G(2d,p)	PMP2/ 6-311+ G(2d,p)	B3LYP/ 6-311+ G(3df,2p)	B3-PMP2/ 6-311+ G(3df,2p)	PMP2/ 6-311+ G(3df,2p)	QCISD(T)/ 6-311+ G(2d,p)	QCISD(T)/ 6-311+ G(3df,2p)
1 → **1**$^{\bullet+}$	889 (9.21)[b]	889 (9.21)	891 (9.23)	893 (9.33)	889 (9.22)	896 (9.32)	910 (9.43)	882 (9.14)	892 (9.24)
1$^{\bullet+}$ → (*E*)-*syn*-HN=CH−CH=C=O$^{\bullet+}$ + HNCO	193	172	168	165	169	172	175	174	184
1$^{\bullet+}$ → (*E*)-*anti*-HN=CH−CH=C=O$^{\bullet+}$ + HNCO	203	182	182	182	179	186	192	191	201
1$^{\bullet+}$ → **11**$^{\bullet}$ + H$^+$	833	834	827	821	837	829	822	833	834
1$^{\bullet+}$ → **12**$^{\bullet}$ + H$^+$	918	918	921	925	920	922	924		
1$^{\bullet+}$ → **13**$^{\bullet}$ + H$^+$	916	916	908	900	916	906	896		
1$^{\bullet+}$ → **14**$^{\bullet}$ + H$^+$	887	888	881	875	887	879	870		
16$^+$ → **1**$^{\bullet+}$ + H$^{\bullet}$	431	427	424	421	430	431	432	421	432
17$^+$ → **1**$^{\bullet+}$ + H$^{\bullet}$	369	366	366	367	370	374	378	368	379
18$^+$ → **1**$^{\bullet+}$ + H$^{\bullet}$	351	348	349	351	347	351	354	356	360
1$^{\bullet+}$ + CH_3SH → **16**$^+$ + $CH_3S^{\bullet}$	−86	−81	−85	−90	−82	−88	−94	−80	−85
1$^{\bullet+}$ + CH_3SH → **18**$^+$ + $CH_3S^{\bullet}$	−6	−2	−11	−20	0.7	−8	−17	−15	−13
1$^{\bullet+}$ + C_6H_5OH → **16**$^+$ + $C_6H_5O^{\bullet}$	−86	−84	−77	−70	−84	−76	−69	−64	−63
1$^{\bullet+}$ + $H_2NCH_2CONHCH_3$ → **16**$^+$ + $H_2NCH^{\bullet}CONHCH_3$	−113	−113	−109	−104	−119	−116	−114	−92	−103
11$^{\bullet+}$ CH_3SH → **11** + $CH_3S^{\bullet}$	−64	−58	−64	−70	−60	−67	−75	−62	−67
12$^{\bullet}$ + CH_3SH → **1** + $CH_3S^{\bullet}$	−149	−142	−158	−174	−143	−160	−177		
13$^{\bullet}$ + CH_3SH → **1** + $CH_3S^{\bullet}$	−146	−140	−145	−149	−139	−144	−149		
14$^{\bullet}$ + CH_3SH → **1** + $CH_3S^{\bullet}$	−118	−112	−118	−124	−110	−117	−123	−116	−115
11$^{\bullet}$ + C_6H_5OH → **1** + $C_6H_5O^{\bullet}$	−64	−61	−55	−50	−61	−55	−49	−45	−45
11$^{\bullet}$ + $H_2NCH_2CONHCH_3$ → **1** + $H_2NCH^{\bullet}CONHCH_3$	−90	−91	−88	−84	−97	−95	−94	−74	−84
14$^{\bullet}$ + CH_3SSCH_3 → **15** + $CH_3S^{\bullet}$	−112	−101	−119	−137	−99	−114	−129		

[a] In units of kJ mol^{-1} at 0 K unless stated otherwise. [b] Adiabatic ionization energies in electronvolts.

Figure 1). Structure **2**$^{\bullet+}$ was the second most stable uracil ion tautomer and was only 8−10 kJ mol^{-1} less stable than **1**$^{\bullet+}$. Structure **2**$^{\bullet+}$ differed from that of neutral tautomer **2** in the lengths of several bonds, as highlighted in Figure 2. These changes upon ionization can be visualized by a combination of canonical structures that indicate shortening of the C-2−N-3, C-2−O-2, and N-1−C-6 bonds and lengthening of the C-5−C-6 and N-1−C-2 bonds (Figure 2). The structures of the less stable tautomers **3**$^{\bullet+}$−**7**$^{\bullet+}$ showed similar changes in bond lengths upon ionization, as summarized in Figure 3. Finally, tautomers **8**$^{\bullet+}$−**10**$^{\bullet+}$ (Figure 4) in which the ring π-electron system was interrupted by the C-5 methylene group were substantially less stable than **1**$^{\bullet+}$. The relative energies of uracil cation radical tautomers, as calculated by several levels of theory, are summarized in Table 1. Cation radical (**1**$^{\bullet+}$) is known to be an intrinsically stable species in the gas phase, as evidenced by the electron ionization mass spectrum of uracil that shows an abundant molecular ion for **1**$^{\bullet+}$.[18] According to the present calculations, the lowest energy unimolecular dissociation of **1**$^{\bullet+}$ to form (*E*)-*syn*-HN=CH−CH=C=O$^{\bullet+}$ + HN=C=O required 184 kJ mol^{-1} at 0 K. A geometrical isomer, (*E*)-*anti*-HN=CH−CH=C=O$^{\bullet+}$, was 17 kJ mol^{-1} less stable than the (*E*)-syn isomer, and hence its formation should have a correspondingly higher dissociation threshold (Scheme 1). Note that HN=CH−CH=C=O$^{\bullet+}$ (*m*/*z* 69) is the dominant product of unimolecular dissociation of **1**$^{\bullet+}$.[18] The substantial threshold energy for the most favorable unimolecular dissociation indicated that thermal **1**$^{\bullet+}$ should be intrinsically stable over a broad temperature range.

SCHEME 1

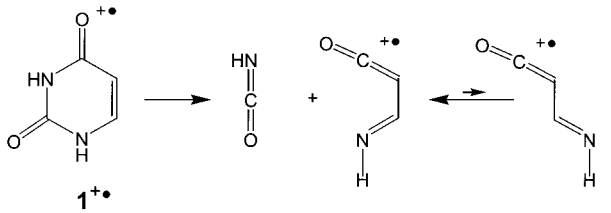

SCHEME 2

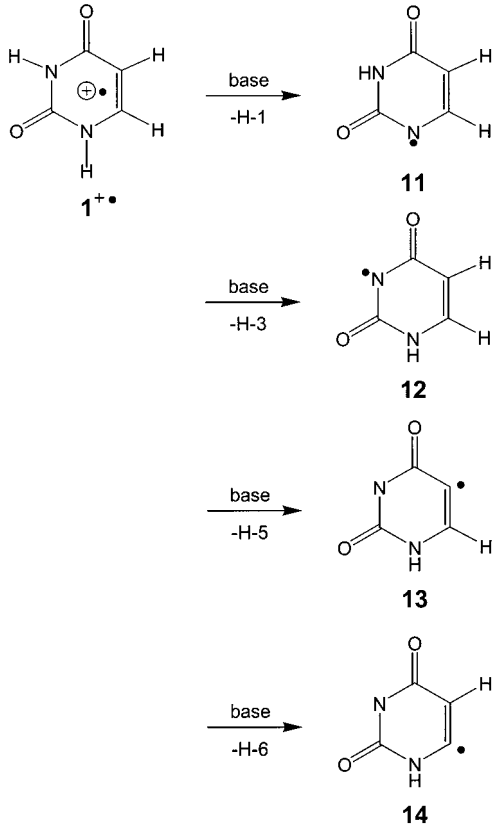

Perhaps most importantly, the stability of $\mathbf{1}^{\bullet+}$ relative to the other tautomers implied that ion−molecule reactions of thermal species should not involve tautomerizations that would be catalyzed by the neutral molecule, as observed previously for other systems.[19] The calculated gas-phase equilibrium involving $\mathbf{1}^{\bullet+}$ and the second most stable tautomer $\mathbf{2}^{\bullet+}$ showed predominant population of $\mathbf{1}^{\bullet+}$, e.g., 97−99% and 89−93% at 298 and 523 K, respectively, depending on the computational method. It is worth noting that the energy difference for $\mathbf{1}^{\bullet+} \rightarrow \mathbf{2}^{\bullet+}$ (8−10 kJ mol^{-1}, Table 1) was substantially smaller than that for the corresponding neutral molecules $\mathbf{1} \rightarrow \mathbf{2}$ (46 kJ mol^{-1}).[17b] This was consistent with the well-known stabilization of enol moieties in cation radicals compared with the corresponding oxo forms.[20] However, in uracil ions the stabilization of the enol forms was not large enough to result in a reversal of ion relative stabilities, so the oxo form $\mathbf{1}^{\bullet+}$ remained the most stable tautomer.

Ion−Molecule Reactions of $\mathbf{1}^{\bullet+}$. The energetics of uracil cation radicals, as discussed above, indicated that ions formed by ionization of uracil have structure $\mathbf{1}^{\bullet+}$ and are stable in an isolated state. Because of the cationic and radical nature of $\mathbf{1}^{\bullet+}$, its ion−molecule reactions may involve electron, proton, hydride, hydrogen atom, or larger radical transfer. The relatively high ionization energy of **1** makes the cation radical $\mathbf{1}^{\bullet+}$ a reactive species for charge-transfer ionization of neutral molecules. The calculated adiabatic ionization energy of **1**, IE_a = 9.24 and 9.32 eV from QCISD(T) and B3-PMP2 calculations, respectively (Table 2), was in very satisfactory agreement with the experimental determinations from photoelectron spectra. Note that accurate measurements of IE_a(**1**) were made difficult by the gradual onset of the first band in the photoelectron spectrum, so that the reported values, 9.2 [21] and 9.34 eV,[22] practically coincide with the IE_a calculated at different levels of theory in this work. Regardless of the most accurate value for the IE_a for uracil, the 9.2−9.3 eV figure indicates that a number of molecules considered for proton or other transfer reactions with $\mathbf{1}^{\bullet+}$ can undergo competitive charge-transfer ionization. Investigation of the kinetics of such competitive reactions is beyond the scope of the present work.

Proton-Transfer Reactions. The kinetics of proton transfer in thermal gas-phase ion−molecule reactions is governed by the reaction energetics,[23] such that only exothermic and nearly thermoneutral reactions are typically observed at low pressure.[24] Ion $\mathbf{1}^{\bullet+}$ has four chemically different protons, H-1, H-3, H-5, and H-6, that can be transferred onto a base in the course of an ion−molecule reaction to form uracil radicals $\mathbf{11}^{\bullet}$, $\mathbf{12}^{\bullet}$, $\mathbf{13}^{\bullet}$, and $\mathbf{14}^{\bullet}$, respectively (Scheme 2). The propensity for proton transfer can be gauged by the topical acidities[25] of H-1, H-3, H-5, and H-6, as summarized in Table 2. The ordering of the topical acidities in $\mathbf{1}^{\bullet+}$ followed the relative stabilities of uracil radicals $\mathbf{11}^{\bullet}$−$\mathbf{14}^{\bullet}$, which were the corresponding deprotonation products. Out of these, radical $\mathbf{11}^{\bullet}$ was substantially more stable than $\mathbf{12}^{\bullet}$, $\mathbf{13}^{\bullet}$, and $\mathbf{14}^{\bullet}$, such that H-1 was the most acidic proton in $\mathbf{1}^{\bullet+}$ of ΔH_{acid} = 829 kJ mol^{-1} (Table 2). This, when compared with the known proton affinities (PA) of organic molecules,[18] implied that $\mathbf{1}^{\bullet+}$ can exothermically transfer H-1 onto amine, amide, and sulfide groups in amino acids and peptides, as well as onto basic heterocycles in histidine and tryptophan. The importance for proton transfer of the less acidic protons H-3, H-5, and H-6 may arise in reactions of uridine and deoxyuridine in which H-1 is substituted by a ribosyl or 2-deoxyribosyl moiety. Note that H-6 is sufficiently acidic to protonate aliphatic amine groups and N-substituted amide groups in peptides, an imidazole ring in histidine, and an indole ring in tryptophan, but not the less basic hydroxyl, thiol, sulfide, disulfide, carboxyl, carboxamide, and phenyl residues in the side chains of serine, cysteine, methionine, cystine, aspartic and glutamic acids, asparagine and glutamine, and phenylalanine and tyrosine, respectively. Likewise, nucleobase residues adenine (PA = 943 kJ mol^{-1}), guanine (PA = 960 kJ mol^{-1}), and cytosine (PA = 950 kJ mol^{-1})[18] are sufficiently basic to be exothermically protonated by any of the acidic protons in $\mathbf{1}^{\bullet+}$. In summary, ion $\mathbf{1}^{\bullet+}$ represents an acid that can protonate a variety of sites in nucleic acids and proteins.

Radical Reactions of Deprotonated $\mathbf{1}^{\bullet+}$. Radicals $\mathbf{11}^{\bullet}$−$\mathbf{14}^{\bullet}$ formed from $\mathbf{1}^{\bullet+}$ upon deprotonation are potentially reactive species that can further react with a suitable substrate and thus propagate the radiation damage from the nucleic acid to another biomolecule. The reactions considered here are hydrogen atom abstractions and transfer of larger functional groups onto the uracil radicals. Abstraction of the thiol hydrogen atom from cysteine is predicted to be substantially exothermic as judged from the enthalpy of the model reaction with methanethiol, which showed $\Delta H_{r,0}$ = −64 kJ mol^{-1} for $\mathbf{11}^{\bullet}$ (Scheme 3, eq a), and even greater exothermicity for the less stable radicals $\mathbf{12}^{\bullet}$−$\mathbf{14}^{\bullet}$ (Table 2). The hydrogen transfer in eq a may require a small activation energy (5−10 kJ mol^{-1}) similar to those in analogous hydrogen atom abstraction reactions.[26] The magnitude of the activation barrier was not addressed in the present calculations. Abstraction of the hydroxyl hydrogen atom from a tyrosine

SCHEME 3

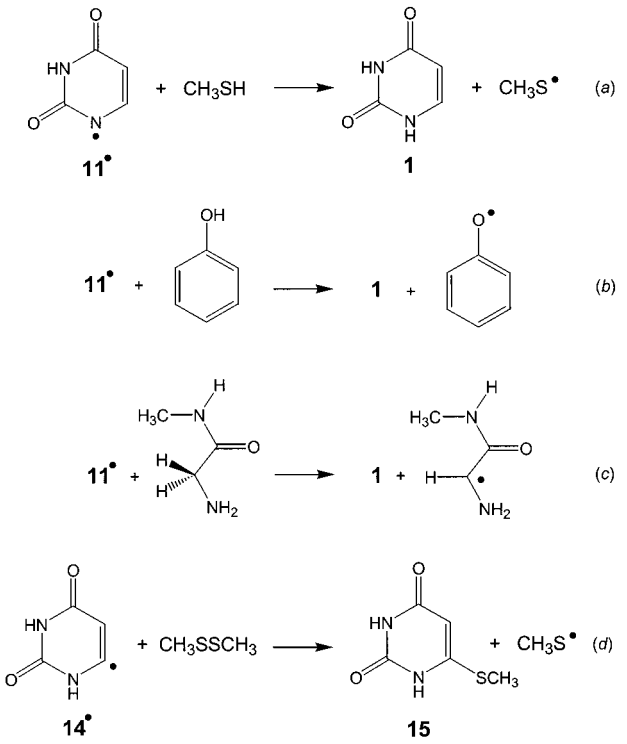

SCHEME 4

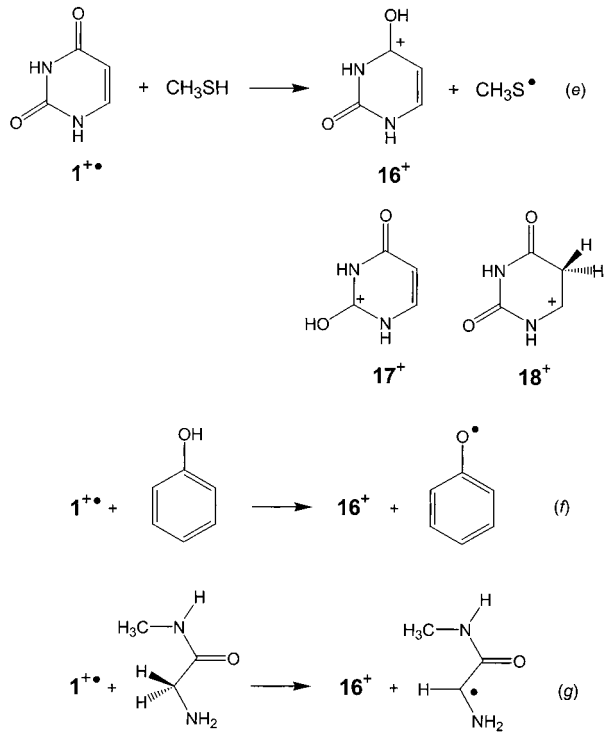

residue is predicted to be also substantially exothermic, when based on the enthalpies of reactions with phenol (Scheme 3, eq b; Table 2). The thermochemistry of reactions of uracil radicals with peptide backbone α-hydrogen atoms was modeled for glycine *N*-methylamide, which showed $\Delta H_{r,0} = -95$ kJ mol^{-1} for **11**$^{\bullet}$ (Scheme 2, eq c) and correspondingly higher exothermicities for the less stable radicals **12**$^{\bullet}$−**14**$^{\bullet}$. Consistent with the gas-phase reactivity of radicals to CH_3S transfer from dimethyl disulfide,[27] the reaction of **14**$^{\bullet}$ was calculated to be substantially exothermic to yield 6-methylthiouracil (**15**, Scheme 3, eq d, Table 2).

Radical Transfer to 1$^{\bullet+}$**.** In addition to electron and proton transfer, cation radical **1**$^{\bullet+}$ can abstract a hydrogen atom or another radical from a suitable donor. The topical hydrogen atom affinities of O-2, O-4, and C-5 and pertinent enthalpies for model reactions are summarized in Table 2. Note that hydrogen atom addition to C-6 in **1**$^{\bullet+}$ would result in an intrinsically unstable cation **19**$^{+}$.[17b] Transfer of a thiol hydrogen atom onto O-4 in **1**$^{\bullet+}$ is a highly exothermic reaction forming cation **16**$^{+}$, as illustrated in Scheme 4 (eq e). Cation **16**$^{+}$ is the most stable isomer among the tautomers of protonated uracil.[17b] Moreover, H-atom transfers to O-2 (forming **17**$^{+}$) and C-5 (forming **18**$^{+}$) were calculated to be also exothermic and therefore energetically possible in the gas phase. Hence, hydrogen abstractions by **1**$^{\bullet+}$ can be expected to exhibit low regiospecificity in forming ions **16**$^{+}$, **17**$^{+}$, and **18**$^{+}$. Not too surprisingly, **1**$^{\bullet+}$ was also calculated to abstract the hydroxyl hydrogen from phenol to form **16**$^{+}$ and a phenoxy radical (Scheme 4, eq f) and an α-hydrogen from glycine *N*-methylamide to form **16**$^{+}$ and an α-glycyl radical (Scheme 4, eq g). It is interesting to note in this context that, according to the calculated bond dissociation energies in glycine,[28] transfer to **1**$^{\bullet+}$ of an amine hydrogen atom is expected to be nearly thermoneutral, while transfer of the hydrogen atom from the carboxylic group should be endothermic.

Properties and Reaction Energetics of Uracil Anion Radical. Uracil has a very low electron affinity (EA) that was determined experimentally from two measurements as 0.02 and 0.04 eV.[29,30] A vertical value on the order of 0.2 eV has recently been estimated from electron scattering studies.[31] The nature of electron bonding in **1**$^{\bullet-}$ was discussed extensively, and both a dipole-bound structure[29,32] and a true local energy minimum have been suggested.[33−37] The most recent density functional theory calculations by Wetmore et al.[38] and Wesolowski et al.[39] indicated a positive electron affinity for uracil on the order of 0.1−0.2 eV. The present calculations using the B3-PMP2 scheme balance the positive values from B3LYP[39] energies with the negative contributions from PMP2 energies to give EA(**1**) = 0.04 eV (Table 3). It is noteworthy that increasing the basis set in the perturbational treatment and extrapolating to effective QCISD(T)/6-311+G(3df,2p) energies increases EA(**1**) to −0.07 eV (Table 3), yet does not result in a positive value. It should be further noted that the B3-PMP2 electron affinity of uracil decreased from 0.04 eV at 0 K to 0.02 eV at 298 K. This implied that **1**$^{\bullet-}$ should be extremely susceptible to thermally induced electron detachment even at room temperature. The low stability of uracil anion radicals is further documented by an enol tautomer (**2**$^{\bullet-}$) which was 63 kJ mol^{-1} less stable than **1**$^{\bullet-}$ (Table 3). Note that although structure **2**$^{\bullet-}$ represented a potential energy minimum in B3LYP geometry optimizations, it was metastable toward thermal electron detachment, which was 19 kJ mol^{-1} exothermic at 298 K.

The optimized structures of anion radicals **1**$^{\bullet-}$ and **2**$^{\bullet-}$ deserve a brief comment. **1**$^{\bullet-}$ displayed a slightly puckered ring due to pyramidization at C-6 and N-1 (Figure 5). Consequently, H-1 and H-6 lay 31° and 18° out of the planes defined by the C-5−C-6−N-1 and C-6−N-1−C-2 atoms, respectively. The ring in **2**$^{\bullet-}$ was slightly bent by pyramidization at N-3 and C-5, whereby the C-4−O-4 carbonyl bond was pointing above the ring and H-3 and H-5 were below the ring (Figure 6).The relative stabilities of uracil tautomers showed a correlation with electronic structure. Stabilization of the dioxo tautomer, expressed as ΔH_0(**1**→**2**) = 44 kJ mol^{-1}, increased upon adding an electron, e.g., ΔH_0(**1**$^{\bullet-}$→**2**$^{\bullet-}$) = 63 kJ mol^{-1}, but decreased upon electron removal, e.g., ΔH_0(**1**$^{\bullet+}$→**2**$^{\bullet+}$) = 8 kJ mol^{-1}. The increased energy difference between anion radicals **1**$^{\bullet-}$ and **2**$^{\bullet-}$

TABLE 3: Energetics of Uracil Anion radical Reactions

	relative energy[a]								
reaction	B3LYP/ 6-31+ G(d,p)	B3LYP/ 6-311+ G(2d,p)	B3-PMP2/ 6-311+ G(2d,p)	PMP2/ 6-311+ G(2d,p)	B3LYP/ 6-311+ G(3df,2p)	B3-PMP2/ 6-311+ G(3df,2p)	PMP2/ 6-311+ G(3df,2p)	QCISD(T)/ 6-311+ G(2d,p)	QCISD(T)/ 6-311+ G(3df,2p)
$\mathbf{1}^{\bullet-} \rightarrow \mathbf{1}$	19 (0.2)[b]	17 (0.18)	2 (0.02)	−13 (−0.14)	16 (0.17)	4 (0.04)	−8 (−0.08)	−12 (−0.13)	−7 (−0.07)
$\mathbf{2}^{\bullet-} \rightarrow \mathbf{2}$	−2	−2	−17	−32					
$\mathbf{1}^{\bullet-} + CH_3SH \rightarrow \mathbf{18}^{\bullet} + CH_3S^-$	54	60	61	61	64	62	61	61	60
$\mathbf{1}^{\bullet-} + CH_3SH \rightarrow \mathbf{19}^- + CH_3S^{\bullet}$	43	49	41	33	53	45	38	34	38
$\mathbf{1}^{\bullet-} + C_6H_5OH \rightarrow \mathbf{18}^{\bullet} + C_6H_5O^-$	19	21	19	17	23	23	22	15	20
$\mathbf{1}^{\bullet-} + C_6H_5OH \rightarrow \mathbf{19}^- + C_6H_5O^{\bullet}$	42	46	50	53	51	57	63	50	60
$\mathbf{1}^{\bullet-} + CH_3SSCH_3 \rightarrow \mathbf{20}^{\bullet} + CH_3S^-$	67	79	69	58	84	75	65		
$\mathbf{1}^{\bullet-} + CH_3SSCH_3 \rightarrow \mathbf{20}^- + CH_3S^{\bullet}$	28	41	34	28	46	43	41		
$\mathbf{1}^{\bullet-} + H_2NCH_2COOH \rightarrow \mathbf{16}^{\bullet} + H_2NCH_2COO^-$	27	28	28	29	27	27	27	29	27
$\mathbf{1}^{\bullet-} + H_2NCH_2COOH \rightarrow \mathbf{18}^{\bullet} + H_2NCH_2COO^-$	−14	−10	−12	−14	−7	−8	−9	−16	−11
$\mathbf{1}^{\bullet-} + H_2NCH_2COOH \rightarrow \mathbf{19}^{\bullet} + H_2NCH_2COO^-$	−6	−2	−2	−3	2	3	3	−5	1

[a] In units of kJ mol^{-1} at 0 K unless stated otherwise. [b] Adiabatic electron affinities in electronvolts.

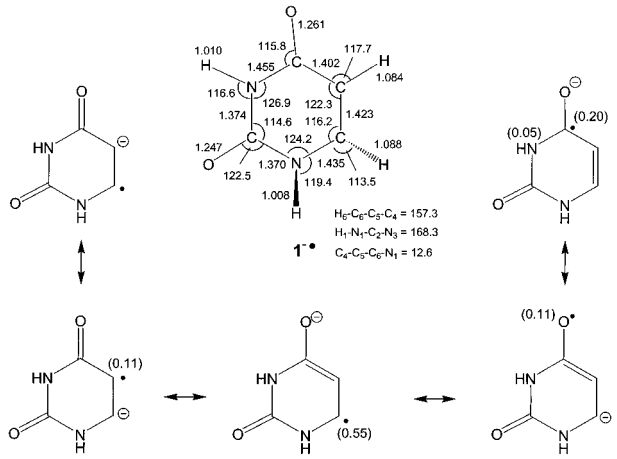

Figure 5. B3LYP/6-31+G(d,p) optimized geometry of $\mathbf{1}^{\bullet-}$. Bond lengths in angstroms, bond and dihedral angles in degrees. Atomic spin densities from B3LYP/6-311+G(2d,p) calculations are shown in parentheses in the canonic structures.

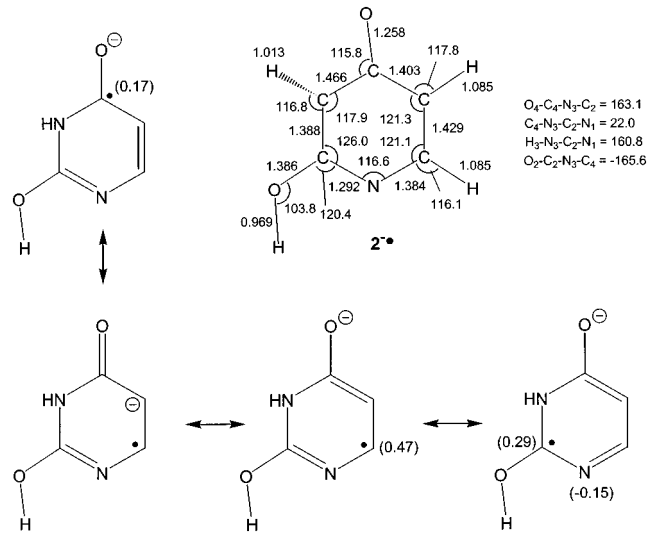

Figure 6. B3LYP/6-31+G(d,p) optimized geometry of $\mathbf{2}^{\bullet-}$. Bond lengths in angstroms, bond and dihedral angles in degrees. Atomic spin densities from B3LYP/6-311+G(2d,p) calculations are shown in parentheses in the canonic structures.

is probably due to electron repulsion effects. The unpaired electron in $\mathbf{1}^{\bullet-}$ is delocalized across the O−C-4−C-5−C-6 enone system, as indicated by the corresponding atomic spin densities that show a maximum value for C-6 (Figure 5). Interestingly, the ureido moiety does not accommodate any substantial spin density in $\mathbf{1}^{\bullet-}$. In contrast, the unpaired electron in $\mathbf{2}^{\bullet-}$ is delocalized over C-2, C-4, and C-6 and thus interacts with the isoureido moiety causing spin polarization at N-1 (Figure 6). Since N-1 carries a substantial negative atomic charge in **2** (−0.45), the electron density flow into the isoureido moiety in $\mathbf{2}^{\bullet-}$ is likely to result in an increased electron repulsion that destabilizes the anion radical.

The 0 K enthalpies of reactions of $\mathbf{1}^{\bullet-}$ with several hydrogen atom and proton donors are summarized in Table 3. The data suggest that $\mathbf{1}^{\bullet-}$ is essentially unreactive toward thiol and phenol groups. Both hydrogen atom and proton transfer from methanethiol and phenol were substantially endothermic and hence disfavored in the gas phase, as shown for the formation of $\mathbf{18}^{\bullet}$ (Table 3) and $\mathbf{19}^-$ (eq h, Scheme 5). Interestingly, the reaction of $\mathbf{1}^{\bullet-}$ by transfer of a methanethiyl radical from dimethyl disulfide to form 6-(methylthio)uracil-5-yl ($\mathbf{20}^{\bullet}$) (eq i) was also endothermic (Table 3), as was the transfer of a methanethiyl anion (eq j, Scheme 5). This implied that $\mathbf{1}^{\bullet-}$ should not show radical-like reactivity in abstracting CH_3S from dimethyl disulfide.[27] The low basicity of $\mathbf{1}^{\bullet-}$ in reactions with CH_3SH and phenol pointed out that one should expect very low acidities for uracil radicals formed by hydrogen atom addition to **1**. A mildly exothermic reaction was calculated for gas-phase transfer onto C-5 in $\mathbf{1}^{\bullet-}$ of the carboxylic proton from glycine; $\Delta H_{rxn} = -11$ and -12 kJ mol^{-1} at 0 and 298 K, respectively (Table 3). However, O-2, O-4, and C-6 in $\mathbf{1}^{\bullet-}$ were even less basic than C-5, so that proton transfers onto those positions from the glycine carboxylic group were endothermic. This suggested that $\mathbf{1}^{\bullet-}$ could undergo regiospecific gas-phase protonation with glycine or other carboxylic acids to form radical **17**. The calculated topical gas-phase acidities of uracil radicals are summarized in Table 4

TABLE 4: Topical Acidities of Uracil Radicals

	gas-phase acidity[a,b]								
radical	B3LYP/ 6-31+ G(d,p)	B3LYP/ 6-311+ G(2d,p)	B3-PMP2/ 6-311+ G(2d,p)	PMP2/ 6-311+ G(2d,p)	B3LYP/ 6-311+ G(3df,2p)	B3-PMP2/ 6-311+ G(3df,2p)	PMP2/ 6-311+ G(3df,2p)	QCISD(T)/ 6-311+ G(2d,p)	QCISD(T)/ 6-311+ G(3df,2p)
15$^{\bullet}$ → **1**$^{\bullet-}$ + H^+	1387	1390	1386	1382	1393	1389	1384	1392	1394
16$^{\bullet}$ → **1**$^{\bullet-}$ + H^+	1321	1320	1316	1312	1322	1317	1311	1330	1317
17$^{\bullet}$ → **1**$^{\bullet-}$ + H^+	1428	1427	1427	1426	1427	1424	1421	1443	1433
18$^{\bullet}$ → **1**$^{\bullet-}$ + H^+	1420	1415	1417	1419	1418	1413	1408	1426	1420

[a] Defined as the enthalpy of gas-phase dissociation, HA → A^- + H^+. [b] 0 K values in kJ mol^{-1}.

SCHEME 5

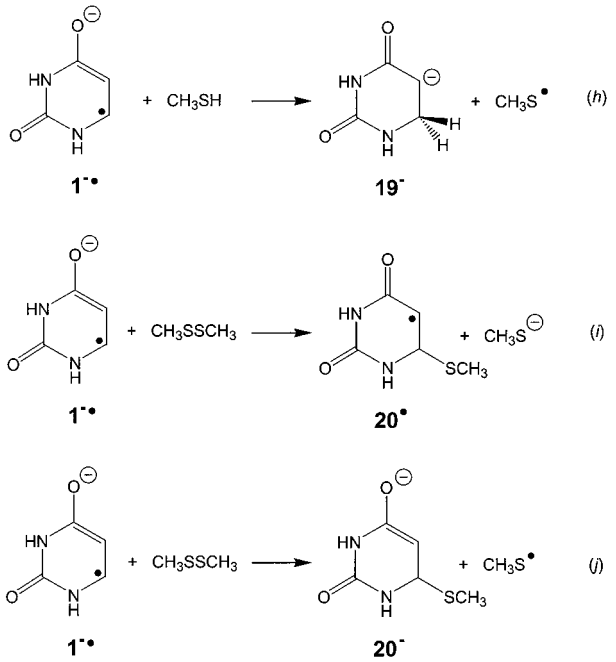

Conclusions

It can be concluded from the present calculations that uracil cation radicals, radicals, and anion radicals differ substantially in the energetics of gas-phase reactions with thiol, phenol, and amino acid α-hydrogens, and the disulfide bond. The uracil cation radical is a very reactive species that is predicted to abstract hydrogen atoms from these groups and also can function as a gas-phase acid to protonate other nucleobases and basic amino acid residues. These reactions may compete with intermolecular electron transfer. Uracil radicals formed by deprotonation of uracil cation radicals have large hydrogen atom affinities and can exothermically abstract hydrogen atoms from thiol groups, phenol, and amino acid α-positions. Proton transfer from the nucleobase followed by hydrogen atom transfer onto the newly formed nucleobase radical is a new possible mechanism for radiation damage following ionization. In contrast, reactions of uracil anion radicals with thiols, phenols, and disulfide bonds are endothermic and hence disfavored in the gas phase. Carboxylic groups can be deprotonated exothermically and possibly selectively by uracil anion radicals.

Acknowledgment. Support of this work by NSF (Grants CHE-9712570 and CHE-0090930) is gratefully acknowledged. The computational facilities used in this work were supported by NSF (Grant CHE-9808182) and the University of Washington.

References and Notes

(1) von Sonntag, C. In *Physical and Chemical Mechanism in Molecular Radiation Biology*; Glass, W. A., Varma, M. N., Eds; Plenum Press: New York, 1991; pp 287−321.

(2) Steenken, S. *Chem. Rev.* **1989**, *89*, 503.

(3) (a) Symons, M. C. R. *J. Chem. Soc., Faraday Trans. 1* **1987**, *83*, 1. (b) Candelas, P.; Steenken, S. *J. Phys. Chem.* **1992**, *96*, 937.

(4) (a) Hwang, C. T.; Stumpf, C. L.; Yu, Y. Q.; Kenttamaa, H. I. *Int. J. Mass Spectrom.* **1999**, *183*, 253. (b) Liu, J.; Crawford, K.; Petzold, C. J.; Kenttamaa, H. I. *Proceedings of the 49th ASMS Conference on Mass Spectrometry and Allied Topics*, Chicago 2001; American Society for Mass Spectrometry: Santa Fe, New Mexico; Presentation No. ThPB 038.

(5) Frisch, M. J.; Trucks, G. W.; Schlegel, H. B.; Scuseria, G. E.; Robb, M. A.; Cheeseman, J. R.; Zakrzewski, V. G.; Montgomery, J. A., Jr.; Stratmann, R. E.; Burant, J. C.; Dapprich, S.; Millam, J. M.; Daniels, A. D.; Kudin, K. N.; Strain, M. C.; Farkas, O.; Tomasi, J.; Barone, V.; Cossi, M.; Cammi, R.; Mennucci, B.; Pomelli, C.; Adamo, C.; Clifford, S.; Ochterski, J.; Petersson, G. A.; Ayala, P. Y.; Cui, Q.; Morokuma, K.; Malick, D. K.; Rabuck, A. D.; Raghavachari, K.; Foresman, J. B.; Cioslowski, J.; Ortiz, J. V.; Stefanov, B. B.; Liu, G.; Liashenko, A.; Piskorz, P.; Komaromi, I.; Gomperts, R.; Martin, R. L.; Fox, D. J.; Keith, T.; Al-Laham, M. A.; Peng, C. Y.; Nanayakkara, A.; Gonzalez, C.; Challacombe, M.; Gill, P. M. W.; Johnson, B. G.; Chen, W.; Wong, M. W.; Andres, J. L.; Head-Gordon, M.; Replogle, E. S.; Pople, J. A. *Gaussian 98*, revision x.x; Gaussian, Inc.: Pittsburgh, PA, 1998.

(6) (a) Becke, A. D. *J. Chem. Phys*, **1993**, *98*, 1372, 5648. (b) Stephens, P. J.; Devlin, F. J.; Chabalowski, C. F.; Frisch, M. J. *J. Phys. Chem.* **1994**, *98*, 11623.

(7) Rauhut, G.; Pulay, P. *J. Phys. Chem.* **1995**, *99*, 3093.

(8) (a) Finley, J. W.; Stephens, P. J. *J. Mol. Struct. (THEOCHEM)* **1995**, *227*, 357. (b) Wong, M. W. *Chem. Phys. Lett.* **1996**, *256*, 391. (c) Scott, A. P.; Radom, L. *J. Phys. Chem.* **1996**, *100*, 16502.

(9) Møller, C.; Plesset, M. S. *Phys. Rev.* **1934**, *46*, 618.

(10) (a) Schlegel, H. B. *J. Chem. Phys.* **1986**, *84*, 4530. (b) Mayer, I. *Adv. Quantum Chem.* **1980**, *12*, 189.

(11) Tureček, F. *J. Phys. Chem. A* **1998**, *102*, 4703.

(12) (a) Tureček, F.; Wolken, J. K. *J. Phys. Chem. A* **1999**, *103*, 1905. (b) Tureček, F.; Carpenter, F. H. *J. Chem. Soc., Perkin Trans. 2* **1999**, 2315. (c) Tureček, F.; Polasek, M.; Frank, A. J.; Sadilek, M. *J. Am. Chem. Soc.* **2000**, *122*, 2361.

(13) Rablen, P. R. *J. Am. Chem. Soc.* **2000**, *122*, 357.

(14) Pople, J. A.; Head-Gordon, M.; Raghavachari, K. *J. Chem. Phys.* **1987**, *87*, 5968.

(15) Curtiss, L. A.; Raghavachari, K.; Pople, J. A. *J. Chem. Phys.* **1993**, *98*, 1293.

(16) (a) Curtiss, L. A.; Redfern, P. C.; Smith, B. J.; Radom, L. *J. Chem. Phys.* **1996**, *104*, 5148. (b) Smith, B. J.; Radom, L. *J. Phys. Chem.* **1995**, *99*, 6468.

(17) (a) Podolyan, Y.; Gorb, L.; Leszczynski, J. *J. Phys. Chem. A* **2000**, *104*, 7346. (b) Wolken, J. K.; Tureček, F. *J. Am. Soc. Mass Spectrom.* **2000**, *11*, 1065. (c) Kryachko, E. S.; Nguyen, M. T.; Zeegers-Huyskens, T. *J. Phys. Chem. A* **2001**, *105*, 1934.

(18) *NIST Standard Reference Database No. 69*; February 2000 Release. http://webbook.nist.gov/chemistry.

(19) (a) Tureček, F.; Drinkwater, D. E.; McLafferty, F. W. *J. Am. Chem. Soc.* **1990**, *112*, 993. (b) Longevialle, P. *Mass Spectrom. Rev.* **1992**, *11*, 157. (c) Audier, H.-E.; Leblanc, D.; Mourgues, P.; McMahon, T. B.; Hammerum, S. *J. Chem. Soc., Chem. Commun.* **1994**, 2329. (d) Mourgues P.; Chamot-Rooke, J.; Nedev, H.; Audier H. E. *J. Mass Spectrom.* **2001**, *36*, 102.

(20) Tureček, F.; Cramer, C. J. *J. Am. Chem. Soc.* **1995**, *117*, 12243. For a review, see: Turecek, F. In *The Chemistry of Enols*; Rappoport, Z., Ed.; Wiley: Chichester, 1990; Chapter 3, pp 95−146.

(21) Yu, C.; O'Donnell, T. J.; LeBreton, P. R. *J. Phys. Chem.* **1981**, *85*, 3851.

(22) Dougherty, D.; Wittel, K.; Meeks, J.; McGlynn, S. P. *J. Am. Chem. Soc.* **1976**, *98*, 3815.

(23) (a) Bouchoux, G.; Salpin, J. Y. *J. Phys. Chem.* **1996**, *100*, 16555. (b) Bouchoux, G.; Salpin, J. Y.; Leblanc, D. *Int. J. Mass Spectrom.* **1996**, *153*, 37.

(24) *Gas-Phase Ion Chemistry*; Bowers, M. T., Ed.; Academic Press: New York, 1979.

(25) Gas-phase acidity (ΔH_{acid}) is defined as the standard enthalpy of dissociation for the reaction $HA \rightarrow A^- + H^+$. See: Lias, S. G.; Bartmess, J. E.; Liebman, J. F.; Holmes, J. L.; Levin, R. D.; Mallard, W. G. *J. Phys. Chem. Ref. Data* **1988**, *17* (Suppl. 1), 6.

(26) See, for example: (a) Atkinson, R. *J. Phys. Chem. Ref. Data*; Monograph No. 2; American Institute of Physics: Woodbury, NY, 1994. (b) Walker, R. W. *Int. J. Chem. Kinet.* **1985**, *17*, 573. (c) Lynch, B. J.; Fast, P. L.; Harris, M.; Truhlar, D. G. *J. Phys. Chem. A* **2001**, *104*, 4811.

(27) Stirk, K. M.; Orlowski, J. C.; Leeck, D. T.; Kenttamaa, H. I. *J. Am. Chem. Soc.* **1992**, *114*, 8604.

(28) Yu, D.; Rauk, A.; Armstrong, D. A. *J. Am. Chem. Soc.* **1995**, *117*, 1789.

(29) Hendricks, J. H.; Lyapustina, S. A.; de Clercq, H. L.; Snodgrass, J. T.; Bowen, K. H. *J. Chem. Phys.* **1996**, *104*, 7788.

(30) Desfrancois, C.; Abdoul-Carime, H.; Scherman, J. P. *J. Chem. Phys.* **1996**, *104*, 7792.

(31) Aflatooni, K.; Gallup, G. A.; Burrow, P. D. *J. Phys. Chem. A* **1998**, 102, 6205.

(32) Adamowicz, L. *J. Phys. Chem.* **1993**, *97*, 11122.

(33) Pullman, B.; Pullman, A. *Rev. Mod. Phys*. **1960**, *32*, 428.

(34) Compton, R. N.; Yoshioka, Y.; Jordan, K. D. *Theor. Chim. Acta* **1980**, *54*, 259.

(35) Younkin, J. M.; Smith, L. J.; Compton, R. N. *Theor. Chim. Acta* **1976**, *41*, 157.

(36) Colson, A.-O.; Besler, B.; Close, D. M.; Sevilla, M. D. *J. Phys. Chem.* **1992**, *96*, 661.

(37) Sevilla, M. D.; Besler, B.; Colson, A.-O. *J. Phys. Chem.* **1995**, *99*, 1060.

(38) Wetmore, S. D.; Boyd, R. J.; Eriksson, L. A. *Chem. Phys. Lett.* **2000**, *322*, 129.

(39) Wesolowski, S. S.; Leininger, M. L.; Pentchev, P. N.; Schaefer, H. F., III. *J. Am. Chem. Soc.* **2001**, *123*, 4023.